

LETTER • OPEN ACCESS

2018 summer extreme temperatures in South Korea and their intensification under 3 °C global warming

To cite this article: Eun-Soon Im *et al* 2019 *Environ. Res. Lett.* **14** 094020

View the [article online](#) for updates and enhancements.

Environmental Research Letters

**OPEN ACCESS****LETTER**

2018 summer extreme temperatures in South Korea and their intensification under 3 °C global warming

RECEIVED
7 March 2019

REVISED
8 August 2019

ACCEPTED FOR PUBLICATION
15 August 2019

PUBLISHED
20 September 2019

Eun-Soon Im^{1,2,4}, Nguyen-Xuan Thanh², Young-Hyun Kim³ and Joong-Bae Ahn^{3,4}

¹ Department of Civil and Environmental Engineering, The Hong Kong University of Science and Technology, Hong Kong, People's Republic of China

² Division of Environment and Sustainability, The Hong Kong University of Science and Technology, Hong Kong, People's Republic of China

³ Division of Earth Environmental System, Pusan National University, Republic of Korea

⁴ Author to whom any correspondence should be addressed.

E-mail: ceim@ust.hk and jbahn@pusan.ac.kr

Keywords: fine-scale climate projections, dynamical downscaling, 2018 Korean heatwaves, regional impacts of global warming, intensified future heat stress

Supplementary material for this article is available [online](#)

Original content from this work may be used under the terms of the Creative Commons Attribution 3.0 licence.

Any further distribution of this work must maintain attribution to the author(s) and the title of the work, journal citation and DOI.

**Abstract**

With the acceleration in global warming, extreme hot temperatures have emerged as one of the most prominent risks. In this study, we characterize the unprecedented extreme temperatures that occurred in Korea in summer 2018, and attempt to explain how this locally observed extreme event can be interpreted in the context of 2 °C and 3 °C global warming above the pre-industrial level. To better resolve geographically diverse climate features and enhance confidence in future changes, three global projections are dynamically downscaled using three regional climate models that are customized over Korea and the systematic biases are statistically corrected using quantile mapping. In July and August 2018, abnormally high maximum temperatures (Tmax) were observed over the entire territory of South Korea. Beyond the increase of mean value, Tmax at individual stations departed significantly from the typical Gaussian distribution of climatological Tmax due to the dramatic changes in the extent and shape of upper tails. The distinct behaviors of Tmax that appeared in 2018 largely represent the statistical analog of the distribution pattern expected under 3 °C global warming based on fine-scale climate projections. This implies that statistically extremely rare events like that of summer 2018 will become increasingly normal if global average temperature is allowed to increase by 3 °C. More importantly, the extreme heat stress measured by the wet-bulb globe temperature is projected to intensify the risks to a level never before seen in contemporary climate. This study is timely and relevant to the need to identify how the globally aggregated warming target temperature can be disaggregated into regional impacts.

1. Introduction

The United Nations Conference on Climate Change (COP21), which was held in Paris in December 2015, reached the consensus that significant efforts need to be made on the reduction of emissions to avoid disastrous consequences attributable to global warming. As a result, the world's governments agreed to keep the increase in global average temperature to well below 2 °C above pre-industrial levels and to ambitiously aim to limit the increase to 1.5 °C

(UNFCCC 2015). Setting out a clear target such as 2 °C warming seems to be an effective way to promote urgency and pursue global actions. On the other hand, it may give the public the wrong perception that the threshold of 2 °C can be regarded as a universally applicable goal and, therefore, that anthropogenic interference with the climate system will remain acceptable until global warming has reached 2 °C. However, any change in global average temperature is not linearly disaggregated into regional and local impacts in a straightforward manner (Knutti *et al* 2016,

Harrington *et al* 2018). In particular, the changes in intensity and frequency of extreme events in response to global average temperature are highly nonlinear at regional scales (Ruff and Neelin 2012).

In summer 2018, South Korea experienced unprecedented extreme hot temperatures over its entire territory. The Korean Meteorological Administration (KMA) reported that record-breaking daily Tmax and consecutive hot days were repeatedly observed in 2018 (KMA 2019). For example, Tmax in Seoul rose to 39.6 °C, which is the highest value ever recorded in the 111 year observational history at that location. Furthermore, Tmax exceeding 40 °C was recorded at Hongchen (41 °C) and Uiseong (40.4 °C), which are unprecedently hot temperatures in Korea. The station-averaged number of heatwaves (defined as Tmax more than 33 °C over 2 d based on the criterion for heatwave advisory issued by the KMA) in Korea in 2018 was 31.4 d (9.8 d of average per year), which is the highest since observations commenced. Not only the maximum temperature, but also the minimum temperature set a new record, with an exceptionally long period of tropical nights (i.e. 17.7 d) compared to the climatological average (i.e. 5.1 d). Although in-depth analysis and further study are required for robust attribution of the observed record-breaking extreme temperatures in 2018, it is probably inexplicable in the absence of any anthropogenic influence. Indeed, Min *et al* (2014) and Kim *et al* (2018) demonstrated the anthropogenic influences on the summer 2013 Korean heatwave using the fraction of attributable risk approach, in which the probability of extreme events occurring is compared in two hypothetical worlds, one without and one with human influences.

Consistent with the projected changes at the global scale such as a virtually certain increase in the frequency and magnitude of unusually warm days and nights (IPCC 2013), recent studies based on climate modeling have demonstrated that the statistical likelihood of extreme hot temperatures and heatwaves in Korea is also projected to increase due to global warming (Lee 2017, Im *et al* 2015, 2017a, Lee and Min 2018, Shin *et al* 2018). Most of these studies have focused on comparative analysis to show how much future climate in response to enhanced greenhouse gas emissions (GHGs) will depart from the reference climate in response to historical GHGs. However, the changing magnitude of temperature in the far future appears to be abstract and ambiguous for non-climate experts. The historical events, which had left drastic impacts, but will be a close analog to future extremes, may help improve the public recognition of the risks in a changing climate (Fitzpatrick and Dunn 2019). In this regard, characterizing the 2003 European heatwaves and identifying their statistical analog from future projections have successfully demonstrated the perception and potential threats of ‘a shape of things to come’ under anthropogenic warming (Beniston 2004, Beniston and Diaz 2004, Schär *et al* 2004, Stott *et al* 2004,

Russo *et al* 2014, Bador *et al* 2017). For the Korean region, the 2018 summer extreme temperature is an excellent example that enables an estimation to be made of the severity of extreme events expected from different levels of global warming. In this study, we investigate the characteristics of the 2018 Korean extreme hot temperatures and compare their departure from the observational climatological normal with projected changes under 2 °C and 3 °C warmer climate conditions based on the state-of-the-art climate simulations that were generated using general circulation models (GCMs), regional climate models (RCMs) and statistical bias correction (quantile mapping). This analysis promises to explain how the unprecedentedly extreme temperatures that appeared in the observational record at the local scale can be interpreted in the context of the 2 °C and 3 °C global warming. Since the 2015 Paris Agreement, a significant body of research has quantified the impact of different levels of warming specified by the various thresholds of global average temperature (e.g. 1.5 °C, 2 °C, 3 °C) (King and Karoly 2017, Wang *et al* 2017, Jacob *et al* 2018, Lee and Min 2018, Lee *et al* 2018, Li *et al* 2018, Sylla *et al* 2018). However, most of these studies applied the GCM projections with relatively coarse resolution, which is not appropriate for investigating detailed features at the regional to local scales. Studies based on dynamically downscaled projections using RCMs with higher resolution were mostly focused on the European region or a few other regions. To the best of our knowledge, Lee and Min (2018) is the only attempt to quantify the future changes in heat stress over Korea, which is centered on their study region of East Asia, under 1.5 °C and 2 °C target temperature conditions. Their study clearly revealed the mitigation benefit of half a degree less warming in terms of heat stress measured by the wet-bulb globe temperature (WBGT). However, a GCM-based result could not provide the details of localized pattern over Korea where the region-specific climate is largely influenced by complicated geographical features. For example, the Taebaek Mountains extending from north to south along the east coast of Korea distinctly differentiates the climate characteristics of the inland mountainous region from the eastern coastal region, despite their separation of less than 50 km. The GCM projections fail to capture such a spatial variability of climate variables over short distances (Qiu *et al* 2019, Lee *et al* 2019a). In particular, since the precise representation of elevation not only in mountainous regions, but also in low-lying basins, critically contributes to the accuracy of temperature simulation, RCM with higher resolution better resolves the sharp gradients of temperature variation and reduces the systematic biases (Qiu *et al* 2019). This study based on dynamically downscaled projections with greater regional details provides a better picture of the local-scale severity of extreme temperatures and resultant heat stress that remains poorly understood. A particular focus is given to the comparison of statistical behaviors between the temperatures

Table 1. Central years and averaged periods corresponding to the 0.48 °C, 2 °C, and 3 °C global warming derived from GCM projections forced by RCP8.5 scenario. The years marked by an asterisk indicate the starting or ending years that do not cover the full of 30-year period.

Target warming	RCM	RegCM4	RegCM4	WRF	SNU-MM5
	GCM	MPI-ESM-MR	NorESM1-M	HadGEM2-AO	HadGEM2-AO
Reference (0.48 °C)	Central year	1978	1991	1991	1991
	Period	1964–1993	1977–2005*	1981*–2005	1981*–2005
	Length	30-year	29-year	26-year	26-year
Future (2 °C)	Central year	2038	2048	2042	2042
	Period	2024–2053	2034–2063	2028–2057	2028–2057
	Length	30-year	30-year	30-year	30-year
Future (3 °C)	Central year	2060	2073	2061	2061
	Period	2046–2075	2059–2088	2047–2076	2047–2076
	Length	30-year	30-year	30-year	30-year

observed in 2018 summer and those projected under a 2.0 °C and 3 °C warmer world. This comparison will have important implications for conceptualizing unexperienced future phenomenon and will help build upon previous findings. This is a timely study that identifies regionally emerging challenges faced by globally targeted warming and that will support the development of better adaptation strategies.

2. Experimental design and analysis method

For fine-scale climate information focusing on the Korean peninsula, three GCM projections were dynamically downscaled using three RCMs (see table 1). The Weather Research and Forecasting (WRF) and Seoul National University Mesoscale Model version 5 (SNU MM5, Cha and Lee 2009) with 12.5 km horizontal resolution were used for the dynamical downscaling of the Hadley Centre Global Environmental Model version 2—Atmosphere and Ocean (HadGEM2-AO). Baek *et al* (2013) demonstrated that HadGEM2-AO showed reasonable performance over East Asia, including our target domain. These two downscaled results are part of the national downscaling project in South Korea, and their detailed configuration and basic performance appear in Im *et al* (2015, 2017a). On the other hand, the Regional Climate Model version 4 (RegCM4, Giorgi *et al* 2012) with 20 km horizontal resolution was used for the dynamical downscaling of the Max Planck Institute for Meteorology Earth System Model-Mixed Resolution (MPI-ESM-MR, Giorgetta *et al* 2013) and Norwegian Earth System Model (NorESM1-M, Bentsen *et al* 2013). These two global projections are guided to give the highest priority of downscaling by the CORDEX Coordinated Output for Regional Evaluations (CORE) program (<http://cordex.org/experiment-guidelines/cordex-core/>). These global projections from HadGEM2-AO, MPI-ESM-MR, and NorESM1-M were forced by the representative concentration pathway (RCP8.5) that is equivalent to the business-as-usual

emission scenario within the framework of the Coupled Model Intercomparison Project phase 5 (CMIP5; Taylor *et al* 2012).

Since the individual models have their own warming phase in response to emissions forcing, we determine the reference and two future periods that correspond to 0.48 °C, 2 °C, and 3 °C warming over the pre-industrial period (1861–1890), based on the same method used in Sylla *et al* (2018). Long-term observed temperature (HadCRUT.4.6, Morice *et al* 2012) undertaken a 30-year running mean reveals that global average temperature increased by 0.48 °C during 1976–2005 compared to that averaged over the pre-industrial period (Sylla *et al* 2018). The pre-industrial and reference periods were set as 1861–1890 and 1976–2005, respectively, in line with IPCC (2013). Table 1 provides the central years and averaged periods corresponding to 0.48 °C, 2 °C, and 3 °C global warming with respect to individual projections. After finding the year surpassing 0.48 °C, 2 °C, and 3 °C from the 30-year running mean of global average temperature simulated by each projection, that year is assigned as the central year for the 30-year average. This method has the advantage of considering the different sensitivity of GCMs to emission forcing, compared to applying a fixed period (e.g. 1976–2005). For reference simulation, the three projections do not cover the full 30-year period corresponding to 0.48 °C warming. For example, the downscaled results of the HadGEM2-AO projection are available from 1981; therefore only a 26 year simulation is used for representing the reference period. However, since the missing year is a marginal portion, it may not introduce a significant obstacle to establishing the validity of the conclusions presented in this study.

To validate the simulated temperature and calculate the bias correction factor using quantile mapping, we use the 56 *in situ* observational data maintained by the KMA during the 30-year period of 1976–2005 over South Korea (figure 1(a)). To facilitate the comparison with *in situ* observations, an inverse distance weighting (IDW) interpolation method is applied to convert the grid-point data of downscaled simulation into 56

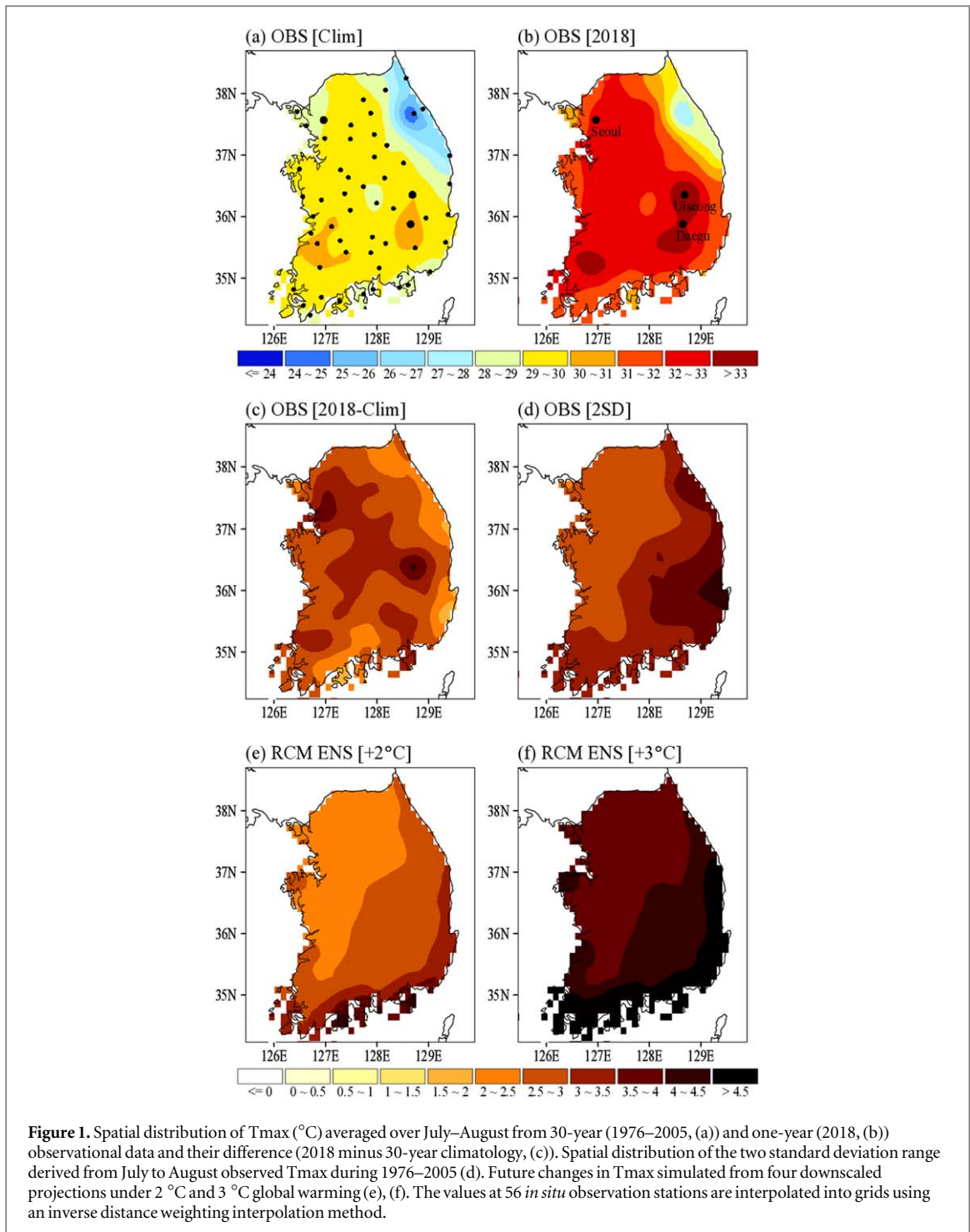


Figure 1. Spatial distribution of T_{max} ($^{\circ}C$) averaged over July–August from 30-year (1976–2005, (a)) and one-year (2018, (b)) observational data and their difference (2018 minus 30-year climatology, (c)). Spatial distribution of the two standard deviation range derived from July to August observed T_{max} during 1976–2005 (d). Future changes in T_{max} simulated from four downscaled projections under $2^{\circ}C$ and $3^{\circ}C$ global warming (e), (f). The values at 56 *in situ* observation stations are interpolated into grids using an inverse distance weighting interpolation method.

stations. The closest four points from the corresponding station are used for the IDW interpolation. In particular, we focus on three stations: Seoul, Uiseong, and Daegu (figure 1(b)). While Seoul and Uiseong experienced extraordinary hot temperatures in summer 2018, Daegu is historically recognized as one of the hottest cities in Korea due to its geographical setting characterized by a low-lying basin surrounded with mountains (Im *et al* 2017a).

Although dynamical downscaling using RCMs can provide added value over driving GCMs in terms of

resolving the heterogeneity of complex geographical features, any climate simulations include unavoidable biases, which reduce the reliability of quantitative estimates in future changes. For example, the extreme analysis counting the exceedance above the absolute threshold may be affected by systematic cold or warm biases. Therefore, statistical bias correction using quantile mapping is applied to remove the systematic bias embedded in the downscaled raw results. The quantile mapping matches the cumulative distribution function (CDF) of raw outputs to observed CDF,

which allows the whole distribution to be effectively adjusted, thereby improving the mean, variance, and extreme values (Lee *et al* 2019b). The Gaussian distribution is used to estimate the probability distribution function for daily Tmax with respect to 56 observational *in situ* stations. A goodness of fit for the estimated distribution for individual stations is verified by the Kolmogorov–Smirnov (K–S) test (Conover 1999), and they are statistically significant at the 95% confidence level for most of stations, which supports the suitability of using the Gaussian distribution for fitting the simulated distributions. To evaluate the bias-corrected reference simulation, the frequency distribution of daily Tmax derived from individual four projections after bias correction and their ensemble means are compared at the station level against *in situ* observation data (figure S1 is available online at stacks.iop.org/ERL/14/094020/mmedia). In addition to the distribution of all 56 stations, three stations (Seoul, Daegu and Uiseong) are individually presented because they are a particular focus in the following analysis. Although individual projections show somewhat different performance, they all are in good agreement with the observed pattern, with the capability to reproduce the present climate. For more quantitative assessments, we provide the metric of the two-sample K–S distance that indicates the maximum distance between two (simulated versus observed) CDFs. Figure S2 presents the K–S distance between simulated and observed daily Tmax distribution for July and August at 56 stations. Daily Tmax distributions for the majority of stations show that their K–S distances do not exceed the critical value at the 99% level, which indicates a certain level of similarity between the simulated and observed distributions. The reasonable performance in capturing the climatological characteristics for the reference period is crucial to enhance the reliability of future climate projections. Under the assumption of ‘stationarity’, which means that the bias pattern does not change with time, the bias correction factor computed from the reference simulation is equally applied to the future projections.

Among the various heat stress indices that measure the combined effects of temperature and humidity, WBGT is used in this study. As presented by table 2 in Willett and Sherwood (2012), WBGT provides a clear threshold to describe the level of risk to physical activity. Due to the unavailability of black globe temperature, we calculate the simplified WBGT, which is an approximation to the WBGT that assumes moderately high radiation levels and light wind conditions. Therefore, the formula to calculate the simplified WBGT includes only temperature and humidity, without accounting for the effect of radiative fluxes and wind (Willett and Sherwood 2012), which is widely accepted (hereafter referred to as WBGT).

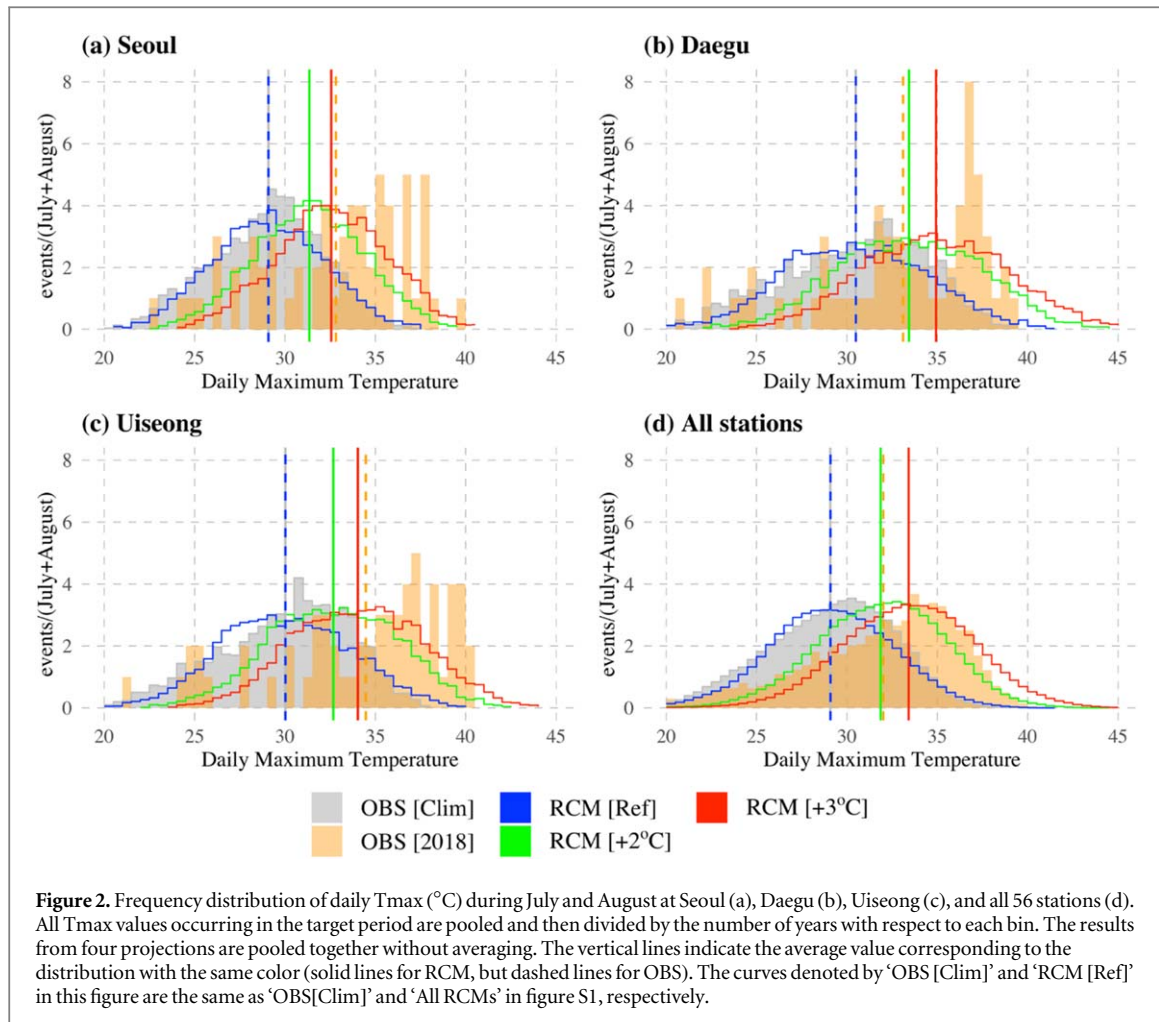
$$\text{WBGT} = 0.567T_a + 0.393e + 3.94$$

$$e = (\text{RH}/100) \times 6.105 \exp\left(\frac{17.27T_a}{237.7 + T_a}\right),$$

where T_a is the surface air temperature ($^{\circ}\text{C}$), e is the vapor pressure (hPa), and RH is the relative humidity (%).

3. Results

We begin our analysis with the spatial distribution of daily Tmax averaged over July and August derived from observational station data: 30-year climatological mean (1976–2005) versus 2018 single year (figures 1(a), (b)). The 56 station data are interpolated into a grid using an IDW interpolation method because the spatial pattern is easily visible from the gridded distribution, but we also provide the same quantity of *in situ* observational sites without any interpolation (figure S3). Comparing these two patterns gives insight into the extent to which 2018 summer deviated from the normal condition. To clearly demonstrate the regional departure pattern from climatology, figure 1 also presents the spatial distribution of the anomaly calculated by subtracting the climatology from 2018 Tmax. In summer 2018, a Tmax anomaly above at least 2°C appears over the entire region of South Korea (figure 1(c)). Such a magnitude of anomalously high temperature is roughly comparable with the plus two standard deviation range of Tmax (figure 1(d)), although the regional pattern shows little consistency between the anomaly and standard deviation. In particular, two localized maxima covering the Seoul and Uiseong stations reach a magnitude of more than 3.5°C (figure 1(c)). To identify the severity of this anomalous pattern, we compare the 2018 Tmax anomaly with the future changes in Tmax derived from the ensemble mean of four downscaled projections (see table 1, hereafter referred to as ENS). Future changes are calculated by the difference between 2°C (3°C) warming and reference periods as denoted in table 1 with respect to four projections individually, and they are then averaged as ENS. The comparison between the 2018 observed anomaly and Tmax increase from future projections demonstrates that the anomalous warming appearing in some regional maxima of summer 2018 already overwhelms the magnitude of the Tmax increase expected under 2°C global warming. Although the 3°C global warming scenario produces a much larger increase of Tmax along the eastern and southern coastal regions, some regions seem to be comparable with those in the 2018 anomalous magnitude. While Tmax averaged over South Korea is projected to increase by 2.7°C under the 2°C target of global average temperature increase, this increment is greatly increased to 4.2°C under 3°C global warming. This implies that regional warming



may not necessarily be estimated by linear scaling from global warming.

On the gross pattern of Tmax averaged over the summer season (e.g. July and August), we examine the frequency distribution of daily Tmax at Seoul, Daegu and Uiseong individual stations, as well as at all 56 stations (figure 2). For this analysis, we pool together all Tmax events occurring during July and August for each bin with empirically chosen intervals of $0.5\text{ }^{\circ}\text{C}$. The frequencies counted for the 30-year period (i.e. OBS Clim) are divided by the number of years (i.e. 30) in order to directly compare the results from a single year (i.e. 2018). For the RCM simulations, the results from four projections are pooled into corresponding bins and the total frequencies are divided by four times the number of years. First, the distribution of Tmax occurring in July and August 2018 differs significantly from the climatological distribution at Seoul, Daegu and Uiseong stations, where extremely high temperatures were observed in summer 2018. Not only is the distribution shifted toward high temperatures, but its shape is also somewhat different from the Gaussian distribution that is normally used to describe the probability of temperature. In particular, the most noticeable feature is found in the upper tails, which probably indicates the occurrence of extreme events. A very

thick and skewed upper tail gives a completely asymmetric shape, which is sufficient to collapse the bell curve of the typical Gaussian distribution. Next, the bias-corrected RCM simulations reasonably capture the characteristics of the Tmax distribution for the reference period, and thus show good agreement with the observed climatological pattern. Individual stations have their own characteristics with different means and variations. For example, compared with the distribution at Daegu, Seoul shows a narrower distribution because of a higher incidence near the mean value and a lower variance. The simulations are capable of capturing these regionally varying statistical behaviors, supporting the necessity of fine-scale climate simulations. The degree of realism achieved in the reference simulation could have important implications for improving the reliability of potential changes in future extreme temperatures. As global warming increases, Korea is likely to suffer unprecedented temperature extremes in the future. Changes in the Tmax distribution clearly demonstrate the shift of both central location and the tail bound in accordance with the degree of warming. Interestingly, the distribution expected under $3\text{ }^{\circ}\text{C}$ global warming largely follows the observed 2018 pattern, even though this single-year pattern shows a somewhat fluctuated

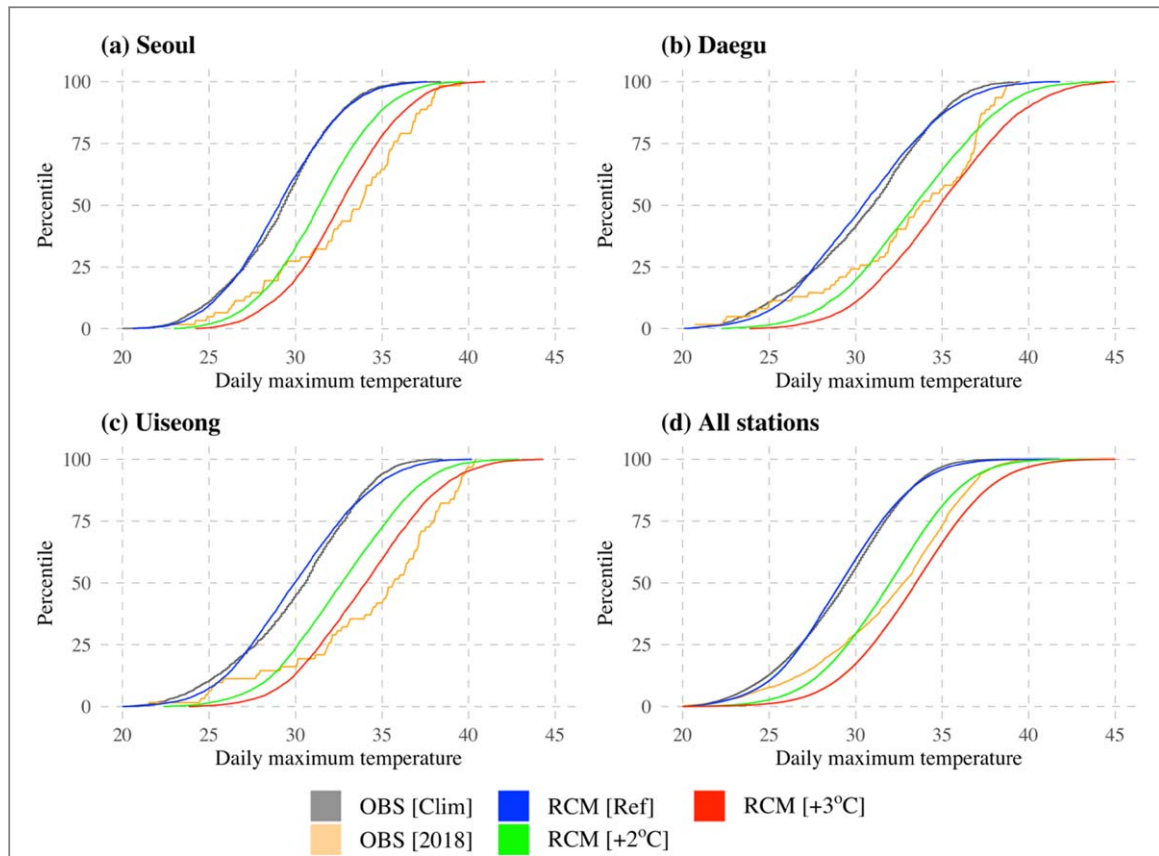


Figure 3. Cumulative distribution function of daily Tmax ($^{\circ}\text{C}$) during July and August at Seoul (a), Daegu (b), Uiseong (c), and all 56 stations (d). The same dataset plotted in figure 2 is used.

shape at particular stations (figures 2(a)–(c)). The distribution from all stations shows stronger similarity between the distribution derived from 2018 Tmax and that expected from $3\text{ }^{\circ}\text{C}$ global warming. This supports that the uncommonly high Tmax under the current climate could become characterized as the new normal in the future if the global average temperature is allowed to increase by up to $3\text{ }^{\circ}\text{C}$. Similar findings have been reported, dealing with climate change issues in the European region (Beniston 2004, Beniston and Diaz 2004, Schär *et al* 2004, Stott *et al* 2004, Russo *et al* 2014).

The unprecedented severity seen in the 2018 extreme temperatures is further explored using the CDF, which readily shows the probability of Tmax exceeding certain thresholds. Figure 3 presents the CDF of Tmax at Seoul, Daegu and Uiseong stations, as well as at all 56 stations derived from observations and RCM simulations. By comparison with the observed climatological pattern, the 2018 CDF exhibits a systematic shift to higher temperatures across all percentiles. The statistical behaviors of Tmax at Seoul and Uiseong stations are particularly relevant. The median CDF values (i.e. the 50th percentile) reach $33.8\text{ }^{\circ}\text{C}$ and $35.7\text{ }^{\circ}\text{C}$ at Seoul and Uiseong in summer 2018, respectively. These are larger than the arithmetic mean values presented in figure 2, and describe a distribution with a negatively skewed shape. The significant changes in median value well explain the

extraordinary nature of the 2018 hot temperatures. More specifically, Tmax at Seoul (Uiseong) during 1976–2005 does not exceed $33.8\text{ }^{\circ}\text{C}$ ($35.7\text{ }^{\circ}\text{C}$), which is the 50th percentile in summer 2018, until the cumulative probability reaches the 95th (97th) percentile. In other words, Tmax occupying the very upper rank (i.e. 5th or 3rd percentile) in the normal condition becomes the central tendency (i.e. 50th percentile) in summer 2018. Consequently, the intensity of extreme heat events, which are typically measured by Tmax exceeding the 95th percentile, also dramatically increases to $38.0\text{ }^{\circ}\text{C}$ and $39.8\text{ }^{\circ}\text{C}$ at Seoul and Uiseong, respectively. In addition, Tmax ranging approximately from the 30th to 95th percentiles largely surpasses that from $3\text{ }^{\circ}\text{C}$ global warming at Seoul and Uiseong, indicating the substantial severity of Tmax in 2018. Moving to the comparison of RCM simulations generated with different levels of increase in global average temperature (i.e. $0.48\text{ }^{\circ}\text{C}$, $2\text{ }^{\circ}\text{C}$ and $3\text{ }^{\circ}\text{C}$), global warming manifests its impacts through shifting the distributions towards higher temperatures compared to the reference climate, which is commonly found in future projections (e.g. Im *et al* 2015). The CDFs under $3\text{ }^{\circ}\text{C}$ global warming at three stations mostly resemble that from summer 2018. Consistent with the frequency distribution in figure 2, this analysis further suggests that the significantly distinct behavior of the 2018 extreme temperatures will probably become the norm in Korea under $3\text{ }^{\circ}\text{C}$ global warming.

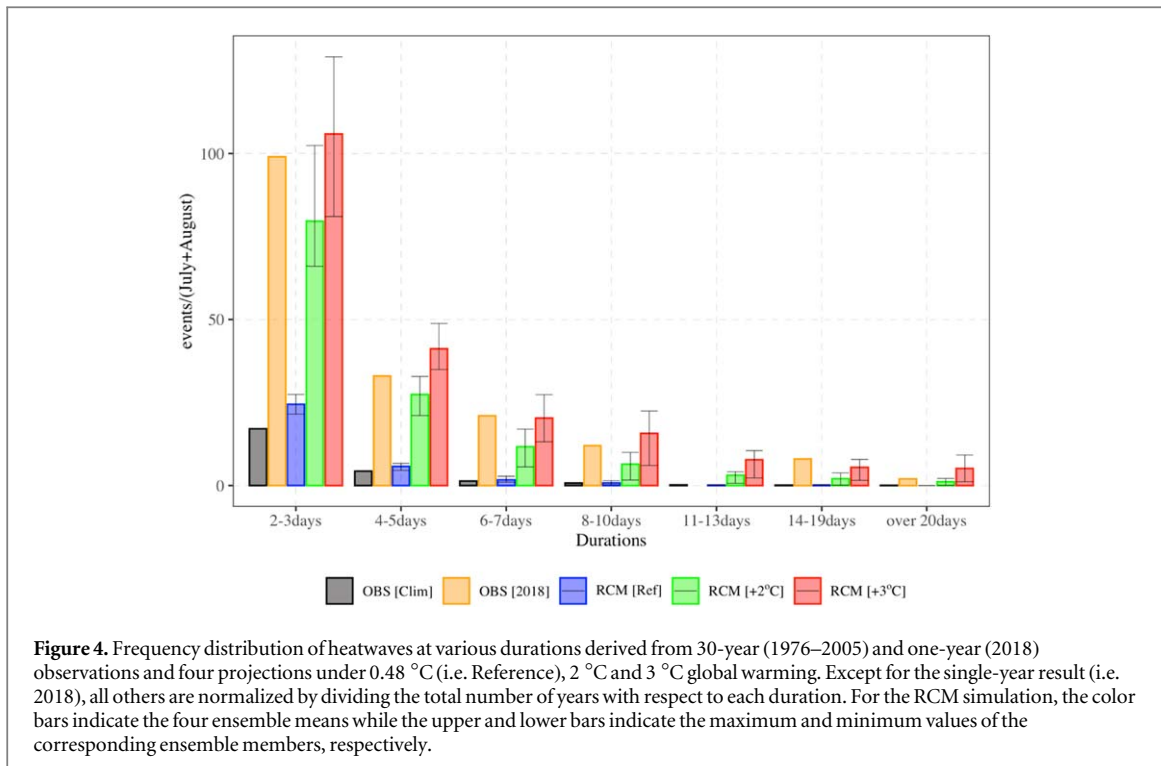
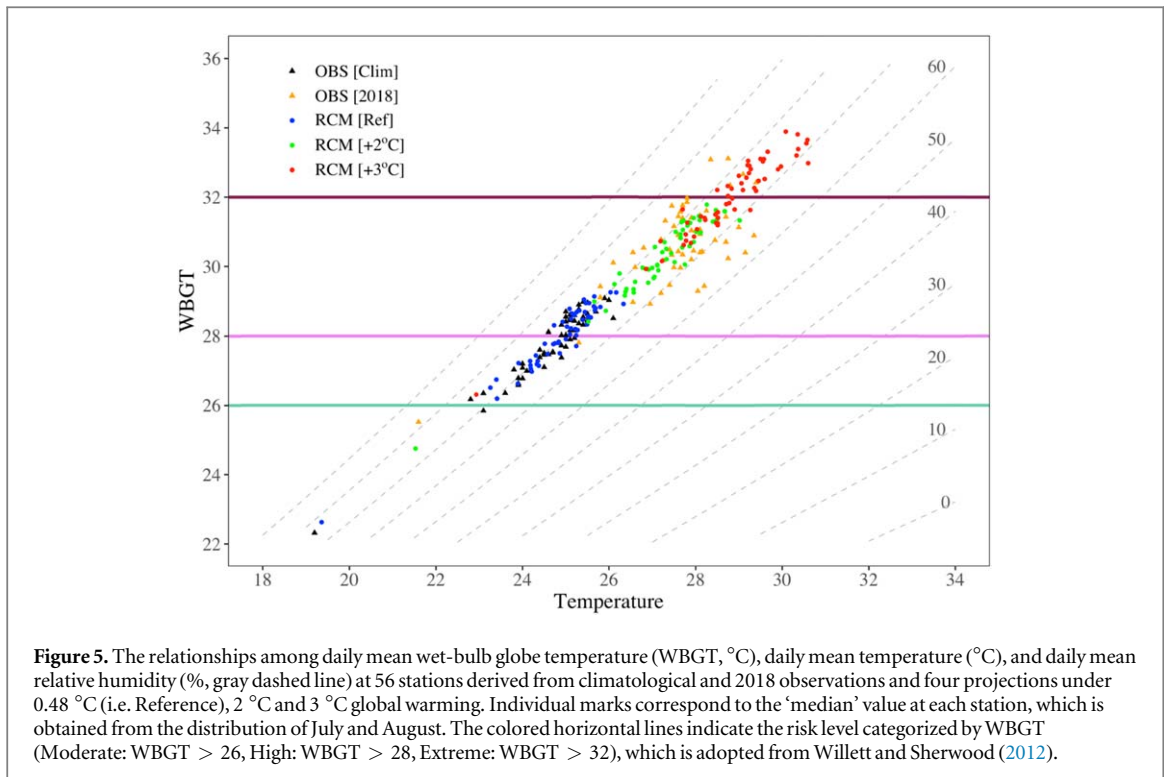


Figure 4. Frequency distribution of heatwaves at various durations derived from 30-year (1976–2005) and one-year (2018) observations and four projections under 0.48 °C (i.e. Reference), 2 °C and 3 °C global warming. Except for the single-year result (i.e. 2018), all others are normalized by dividing the total number of years with respect to each duration. For the RCM simulation, the color bars indicate the four ensemble means while the upper and lower bars indicate the maximum and minimum values of the corresponding ensemble members, respectively.

An increase in temperatures will lead to more frequent and more extended heatwaves. The persistence of extreme hot temperatures can further exacerbate the negative impacts in many sectors (e.g. public health) due to the accumulation of the impacts. Figure 4 presents the frequency distribution of consecutive hot days with Tmax exceeding 35 °C at various durations at 56 stations. The KMA has issued a heatwaves advisory notice and a warning when the daily Tmax is expected to exceed 33 °C and 35 °C for at least 2 d, respectively. Based on this criterion of heatwaves warning, heatwaves with different durations are counted using 62 d (July+August) Tmax for every year at 56 stations. The 2018 observation is the result from only one-year, but others are normalized by dividing the total number of years. For the RCM simulations, the ensemble mean and their spread (formed by maximum and minimum values) of four members are presented. First, the comparison of 2018 with the climatological observed pattern clearly shows the extent to which exceptional heatwaves were experienced during 2018 summer. Second, in spite of some discrepancy, the heatwaves distributions are similar between the climatological (2018) observation and the projection under 0.48 °C (3 °C) global warming. This means that the fine-scale climate simulations used in this study are capable of representing the typical behavior of heatwaves in the present climate, whereas the Korean summer under 3 °C global warming will experience heatwaves as severe as those in 2018 as a norm. A close resemblance between the extreme heatwaves observed in 2018 and those projected under 3 °C global warming is further revealed from the climatological maximum duration of heatwaves

(figure S4). Except for the 2018 case, 30-year observation and RCM projections are averaged over the years and ensemble members after setting the maximum duration of heatwaves for each individual year and individual projection. In particular, the upper extremes projected under 3 °C global warming are likely to be close to the 2018 extreme case. More specifically, the position of several stations as outliers in the box plot from 3 °C global warming projections raise the possibility that the extreme heatwaves, which are considered to have had an unprecedentedly long duration in 2018, could emerge annually.

Among the detrimental consequences of more frequent and intensified extreme hot temperatures, human mortality and morbidity are probably the greatest concern (Son *et al* 2012, Mitchell *et al* 2016). Indeed, the South Korean Ministry of Health, Welfare and Disease Control announced that at least 29 people died due to heatstroke alone in summer 2018, supporting the acutely adverse impact of extreme hot temperatures on human health. From the perspective of health risk, temperature is not the only factor that can affect thermal discomfort and humans' ability to control body temperature. It is also equally important to consider ambient humidity because humans are sensitive to the combination of temperature and humidity (Steinweg and Gutowski 2015, Pal and Eltahir 2016, Im *et al* 2017b). Therefore, we also investigate the characteristics of WBGT that is widely used to measure the heat stress and accompanied risk level (Willett and Sherwood 2012, Im *et al* 2017a, Lee and Min 2018). Figure 5 presents WBGT and daily mean temperature and daily mean relative humidity (RH) used to calculate WBGT. Individual points indicate



the median value obtained from the distribution at each station. For each station, the distribution of 2018 observation is made up of 62 d values while the distribution of climatological observation is made up of 62 d \times 30-year values. WBGT is not computed using daily Tmax because the KMA does not provide the RH data measured when daily Tmax occurs. Since the diurnal cycle of RH is roughly out of phase with temperature, the WBGT calculation using temporally unmatched RH and Tmax might induce a nontrivial error. Therefore, WBGT is calculated using daily mean temperature and daily mean RH, which leads to an underestimation of the heat stress severity compared to WBGT calculated using Tmax and simultaneous RH. Nevertheless, this analysis may well illustrate how the changes in temperature influence the risk arising from heat stress. In general, WBGT and temperature are positively correlated. Therefore, the higher WBGT takes place along the higher temperature accordingly. In Korea's typical summer climate, WBGT mostly ranges from 26 °C to 29 °C, which corresponds to a moderate or marginally high heat stress risk. For summer 2018, the risk level sharply increases and enters the extreme risk category. Although some stations show reduced RH, WBGT is still greatly amplified because the increase in temperature is large enough to offset the effect of reduced RH. Under 3 °C global warming, many more stations are likely to experience extreme risk level, even though some stations are positioned within a similar range with that obtained from the 2018 meteorological condition. The statistics (e.g. median) derived from single-year (62 d) and 30-year (62 d \times 30 years \times 4 members) periods may not agree

perfectly. Although the median is considered to represent the typical value of the distribution, the inter-annual variability during the 30-year period may influence the result. In spite of this caveat, comparing WBGT calculated from the 2018 observational data with RCM projections under 3 °C global warming may help to figure out the specific consequences that a particular region will face due to a certain level of global warming. More importantly, the emergence of far more extreme risks that have never previously arisen in even record-breaking extreme temperatures (e.g. 2018 summer) enables an estimation to be made of the severity of extreme events expected from 3 °C global warming. Most people in Korea will be exposed to severely hazardous summers in terms of heat stress if we fail to limit the global average temperature increase to well below 2 °C above the pre-industrial levels.

4. Discussion and conclusions

It is largely considered that the risks of extreme maximum temperatures and resultant heat stress will continue to increase over many different regions in tandem with the rise in global average temperature (Bador *et al* 2017, Im *et al* 2017a, 2017b, Lee and Min 2018, Sylla *et al* 2018). However, the severity of extreme temperature events at the regional to local scale may not be necessarily proportional to the degree of global warming (Knutti *et al* 2016, Harrington *et al* 2018). Their temporal and spatial patterns still remain uncertain. Since climate change is a global issue with region-specific impacts, it is imperative to quantify the

changes in local temperature in response to the threshold of the globally aggregated target (e.g. 2 °C, 3 °C) in order to better understand the regional consequences of either limiting or allowing further global warming.

In this study, the extraordinary nature of the 2018 extreme hot temperatures is characterized against the climatological observational pattern, and compared with the dynamically downscaled fine-scale climate projections under 2 °C and 3 °C global warming scenarios above the pre-industrial level. The *in situ* observations in July and August 2018 clearly demonstrate substantially higher Tmax across all of South Korea, and the anomalous warmings that appeared in some regions overwhelm the plus two standard deviation range of historical variation of Tmax averaged over July and August. Accordingly, the frequency distribution of Tmax in 2018 departs significantly from the climatological pattern. Both the mean Tmax and the distribution's shape differ substantially from the typical Gaussian fit that is normally applied to describe the behavior of temperature. In particular, the asymmetric distribution with very heavy and skewed upper tail well explains the increase in probability of extreme Tmax. For example, Tmax at Seoul during 1976–2005 does not exceed 35 °C until the cumulative probability reaches about the 98th percentile, whereas Tmax of 35 °C is only positioned at the 64th percentile in summer 2018 because the much higher Tmax is placed in the upper rank. The increase in Tmax directly results in a substantial increase of the frequency and durations of heatwaves. The strong positive relationship observed between Tmax and WBGT indicates that a significant increase in Tmax can induce a high risk of heat stress even when RH is reduced, which is in line with the findings of Im *et al* (2018).

Comparing the 2018 anomalous pattern and future climate projections generated under different levels of global warming gives us a better idea of how to interpret the severity of the 2018 summer extreme temperatures within the context of 2 °C and 3 °C global warming. Locally tailored climate projections obtained through dynamical downscaling and statistical bias correction can capture the geographically diverse characteristic of Tmax over Korea, showing a good agreement with the historical observed pattern. Statistically, the 2018 Tmax and resultant heat stress closely resemble the climate projections expected under the 3 °C global warming scenario. The statistical analog of Tmax between 2018 observations and RCM projections under 3 °C global warming suggests that the unprecedented severity of extreme heat occurring in the current climate could become the future norm unless the increase in global average temperature is stabilized at an acceptable level. A similar conclusion has been drawn from a comparison of the 2003 European heatwaves and future projection in response to elevated GHG forcings (e.g. Beniston 2004, Beniston and Diaz 2004, Schär *et al* 2004, Stott *et al* 2004, Russo *et al* 2014, Bador *et al* 2017).

While characterizing the historical extreme events and assessing the statistical likelihood of future extreme events give insight into the severe impacts of climate change, further in-depth studies are needed to extend our understanding of the physical mechanisms contributing to the changes in intensity and frequency of extreme events. The possible mechanisms behind extreme heatwaves in Korea are complex and have not been fully explored (Kim *et al* 2019). However, the extent and strength of the western North Pacific subtropical high around Korea are often investigated to explain the physical mechanism that is responsible for the heatwaves in South Korea (Yeh *et al* 2018, Yoon *et al* 2018). This is because extreme heatwaves are linked to a specific atmospheric circulation at the synoptic scale (Lee and Lee 2016), even though they are a locally dominating phenomenon. Figure S6 presents the spatial distribution of the historical climatology of the geopotential height at 500 hPa and its anomalous pattern dominated by the year with extreme heatwaves during July and August. The three years with extreme heatwaves under 3 °C global warming that seem to be equivalent to the 2018 case are selected from the temporal evolution of the Tmax anomaly (figure S5). This analysis clearly demonstrates the synoptic framing of the atmospheric condition favorable for heatwaves and the potential of GCM projections to capture these behaviors. In summer 2018, a strong positive anomalous pattern of the geopotential height is found because the significant expansion of the western North Pacific subtropical high to the westward provokes an anomalous anticyclonic circulation over Korea (figure S6(a)). Similarly, the synoptic condition for extreme heatwaves projected under 3 °C global warming is characterized by the enhanced high-pressure system (figure S6(b)), which infers a persistent large-scale subsidence that is favorable for inducing prolonged and intense heatwaves (Lee and Lee 2016). Since the tropospheric warming leads to the greater geopotential height due to the thermal expansion of the atmosphere, the climatology of geopotential height under 3 °C global warming is much higher than that of historical period. Therefore, the anomaly of GCM ENS against historical climatology shows much higher values, compared to observed anomaly of 2018. On the other hand, the magnitude of anomaly against 3 °C warmer climatology is smaller than that of 2018 because the selected extremes are no longer extraordinary ones under 3 °C warmer climate. However, the anomalous spatial pattern of geopotential height expected from extreme heatwaves shows a large similarity with observed one despite some discrepancy in the spatial details (e.g. the position of the maximum). This level of similarity between GCM ENS and ERA-Interim reanalysis is sufficient to support the reliability of GCMs that provide the proper large-scale forcing to the lateral boundary while running RCM. In addition, further research should focus on attributing temperature extremes to

anthropogenic climate change, which will enhance the confidence level of their changed probability under global warming. Very few studies have so far attempted to detect an anthropogenic influence in extreme heatwaves over South Korea or to analyze their attribution to either external forcing or internal climate variability (e.g. Min *et al* 2014).

Although this study has focused on the extreme hot temperatures occurring in Korea, much of our planet suffered a sizzling summer in 2018 with record-breaking temperatures worldwide. The unprecedented 2018 extreme temperatures appears to have enhanced the public awareness of the potentially drastic effects of climate change, beyond being an abstract concept. It should be considered a timely warning of the need for global action to successfully achieve the Paris Agreement on climate change.

Acknowledgments

Im E-S and Nguyen-Xuan T were supported by the Korea Environment Industry & Technology Institute (KEITI) through the Advanced Water Management Research Program, which is funded by the Korea Ministry of Environment (MOE) (Grant 83079). Ahn J-B and Kim Y-H were supported by the Korea Meteorological Administration Research and Development Program under Grant KMI2018-01213.

Data availability statement

The data that support the findings of this study are available from the corresponding author upon reasonable request.

References

- Bador M, Terray L, Boé J, Somot S, Alias A, Gibelin A-L and Dubuisson B 2017 Future summer mega-heatwave and record-breaking temperatures in a warmer France climate *Environ. Res. Lett.* **12** 074025
- Baek H-J *et al* 2013 Climate change in the 21st century simulated by HadGEM2-AO under representative concentration pathways *Asia-Pac. J. Atmos. Sci.* **49** 603–18
- Beniston M 2004 The 2003 heat wave in Europe: a shape of things to come? An analysis based on Swiss climatological data and model simulations *Geophys. Res. Lett.* **31** L02202
- Beniston M and Diaz H F 2004 The 2003 heat wave as an example of summers in a greenhouse climate? Observations and climate model simulations for Basel, Switzerland *Glob. Planet. Change* **44** 73–81
- Bentsen M *et al* 2013 The Norwegian Earth System Model, NorESM1-M: Part I. Description and basic evaluation of the physical climate *Geosci. Model Dev.* **6** 687–720
- Cha D-H and Lee D-K 2009 Reduction of systematic errors in regional climate simulations of the summer monsoon over East Asia and the western North Pacific by applying the spectral nudging technique *J. Geophys. Res.* **114** D14108
- Conover W J 1999 *Practical Nonparametric Statistics* 3rd edn (New York: Wiley) pp 428–33
- Fitzpatrick M C and Dunn R R 2019 Contemporary climatic analogs for 540 North American urban areas in the late 21st century *Nat. Commun.* **10** 614
- Giorgetta M A *et al* 2013 Climate and carbon cycle changes from 1850 to 2100 in MPI-ESM simulations for the coupled model intercomparison project phase 5: climate changes in MPI-ESM *J. Adv. Model. Earth Syst.* **5** 572–97
- Giorgi F *et al* 2012 RegCM4: model description and preliminary tests over multiple CORDEX domains *Clim. Res.* **52** 7–29
- Harrington L J, Frame D, King A D and Otto F E L 2018 How uneven are changes to impact-relevant climate hazards in a 1.5 °C world and beyond? *Geophys. Res. Lett.* **45** 6672–80
- Im E S, Ahn J B and Jo S R 2015 Regional climate projection over South Korea simulated by the HadGEM2-AO and WRF model chain under the RCP emission scenarios *Clim. Res.* **63** 249–66
- Im E S, Choi Y W and Ahn J B 2017a Worsening of heat stress due to global warming in South Korea based on multi-RCM ensemble projections *J. Geophys. Res.: Atmos.* **122** 11444–61
- Im E S, Kang S and Eltahir E A B 2018 Projections of rising heat stress over the western Maritime Continent from dynamically downscaled climate simulations *Glob. Planet. Change* **165** 160–72
- Im E S, Pal J S and Eltahir E A B 2017b Deadly heat waves projected in the densely populated agricultural regions of South Asia *Sci. Adv.* **3** e1603322
- IPCC 2013 Climate change 2013: the physical science basis *Contribution of Working Group I to the Fifth Assessment Report of the Intergovernmental Panel on Climate Change* ed T F Stocker *et al* (Cambridge and New York, NY: Cambridge University Press)
- Jacob D *et al* 2018 Climate impacts in Europe under +1.5 °C global warming *Earth's Future* **6** 264–85
- Kim M K, Oh J S, Park C K, Min S K, Boo K O and Kim J H 2019 Possible impact of the diabatic heating over the Indian subcontinent on heat waves in South Korea *Int. J. Climatol.* **39** 1166–80
- Kim Y-H, Min S-K, Stone D A, Shiogama H and Wolski P 2018 Multi-model event attribution of the summer 2013 heat wave in Korea *Weather Clim. Extremes* **20** 33–44
- King A D and Karoly D 2017 Climate extremes in Europe at 1.5 and 2 degrees of global warming *Environ. Res. Lett.* **12** 114031
- Knutti R, Rogelj J, Sedláček J and Fischer E M 2016 A scientific critique of the two-degree climate change target *Nat. Geosci.* **9** 13–8
- Korea Meteorological Administration 2019 Annual report for 2018 extreme climate pp 1–198 (<https://climate.go.kr/home/bbs/view.php?bname=abnormal&vcode=6232>)
- Lee D, Min S K, Fischer E, Shiogama H, Bethke I, Lierhammer L and Scinocca J F 2018 Impacts of half a degree additional warming on the Asian summer monsoon rainfall characteristics *Environ. Res. Lett.* **13** 044033
- Lee J 2017 Future trend in seasonal lengths and extreme temperature distributions over South Korea *Asia-Pac. J. Atmos. Sci.* **53** 31–41
- Lee M H, Im E S and Bae D H 2019a Impact of the spatial variability of daily precipitation on hydrological projections: a comparison of GCM- and RCM-driven cases in the Han River basin, Korea *Hydrol. Process.* **33** 2240–57
- Lee M H, Im E S and Bae D H 2019b A comparative assessment of climate change impacts on drought over Korea based on multiple climate projections and multiple drought indices *Clim. Dyn.* **53** 389–404
- Lee S M and Min S K 2018 Heat stress changes over East Asia under 1.5° and 2.0 °C global warming targets *J. Clim.* **31** 2819–31
- Lee W S and Lee M I 2016 Interannual variability of heat waves in South Korea and their connection with large-scale atmospheric circulation patterns *Int. J. Climatol.* **36** 4815–30
- Li D, Zhou T, Zou L, Zhang W and Zhang L 2018 Extreme high-temperature events over East Asia in 1.5 °C and 2 °C warmer futures: analysis of NCAR CESM low-warming experiments *Geophys. Res. Lett.* **45** 1541–50
- Min S-K, Kim Y-H, Kim M-K and Park C 2014 Assessing human contribution to the summer 2013 Korean heat wave [in ‘explaining extremes of 2013 from a climate perspective’] *Bull. Am. Meteorol. Soc.* **95** S48–51
- Mitchell D, Heavyside C, Vardoulakis S, Huntingford C, Masato G, Guillod B P, Frumhoff P, Bowery A, Wallom D and Allen M

- 2016 Attributing human mortality during extreme heat waves to anthropogenic climate change *Environ. Res. Lett.* **11** 074006
- Morice C P, Kennedy J J, Rayner N A and Jones P D 2012 Quantifying uncertainties in global and regional temperature change using an ensemble of observational estimates: the HadCRUT4 data set *J. Geophys. Res.: Atmos.* **117** D08101
- Pal J S and Eltahir E A B 2016 Future temperature in southwest Asia projected to exceed a threshold for human adaptability *Nat. Clim. Change* **6** 197–200
- Qiu L, Im E S, Hur J and Shim K M 2019 Added value of very high resolution climate simulations over South Korea using WRF modeling system *Clim. Dyn.* In revision
- Ruff T W and Neelin J D 2012 Long tails in regional surface temperature probability distributions with implications for extremes under global warming *Geophys. Res. Lett.* **39** L04704
- Russo S, Dosio A, Graversen R G, Sillmann J, Carrao H, Dunbar M B, Singleton A, Montagna P, Barbola P and Vogt J V 2014 Magnitude of extreme heat waves in present climate and their projection in a warming world *J. Geophys. Res. Atmos.* **119** 12500–12
- Schär C, Vidale P L, Lüthi D, Frei C, Häberli C, Liniger M A and Appenzeller C 2004 The role of increasing temperature variability in European summer heatwaves *Nature* **427** 332–6
- Shin J, Olson R and An S-I 2018 Projected heat wave characteristics over the Korean Peninsula during the twenty-first century *Asia-Pac. J. Atmos. Sci.* **54** 53–61
- Son J Y, Lee J T, Anderson G B and Bell M L 2012 The impact of heat waves on mortality in seven major cities in Korea *Environ. Health Perspect.* **120** 566–71
- Steinweg C and Gutowski W J 2015 Projected changes in Greater St. Louis summer heat stress in NARCCAP simulations *Weather, Clim. Soc.* **7** 159–68
- Stott P A, Stone D A and Allen M R 2004 Human contribution to the European heatwave of 2003 *Nature* **432** 610–4
- Sylla M B, Faye A, Giorgi F, Diedhiou A and Kunstmann H 2018 Projected heat stress under 1.5 °C and 2 °C global warming scenarios creates unprecedented discomfort for humans in West Africa *Earth's Future* **6** 1029–44
- Taylor K E, Stouffer R J and Meehl G A 2012 An overview of CMIP5 and the experiment design *Bull. Am. Meteorol. Soc.* **93** 485–98
- UNFCCC 2015 Report of the Conf. of the Parties on its twenty-first session *Action taken by the Conf. of the Parties at its 21st session, United Nations (Paris, 30 November to 13 December 2015)* (<http://unfccc.int/resource/docs/2015/cop21/eng/10a01.pdf>)
- Wang Z, Lin L, Zhang X, Zhang H, Liu L and Xu Y 2017 Scenario dependence of future changes in climate extremes under 1.5 °C and 2 °C global warming *Sci. Rep.* **7** 46432
- Willett K M and Sherwood S 2012 Exceedance of heat index thresholds for 15 regions under a warming climate using the wet-bulb globe temperature *Int. J. Climatol.* **32** 161–77
- Yeh S W, Won Y J, Hong J S, Lee K, Kwon M, Seo K H and Ham Y G 2018 The record-breaking heat wave in 2016 over South Korea and its physical mechanism *Mon. Weather Rev.* **146** 1463–74
- Yoon D, Cha D H, Lee G, Park C, Lee M I and Min K H 2018 Impacts of synoptic and local factors on heat wave events over southeastern region of Korea in 2015 *J. Geophys. Res.: Atmos.* **123** 12081–96